by Wencheng Wang,
Xiaohui Yuan, Xiaojin Wu,
Tao Ji, and Lin Feng

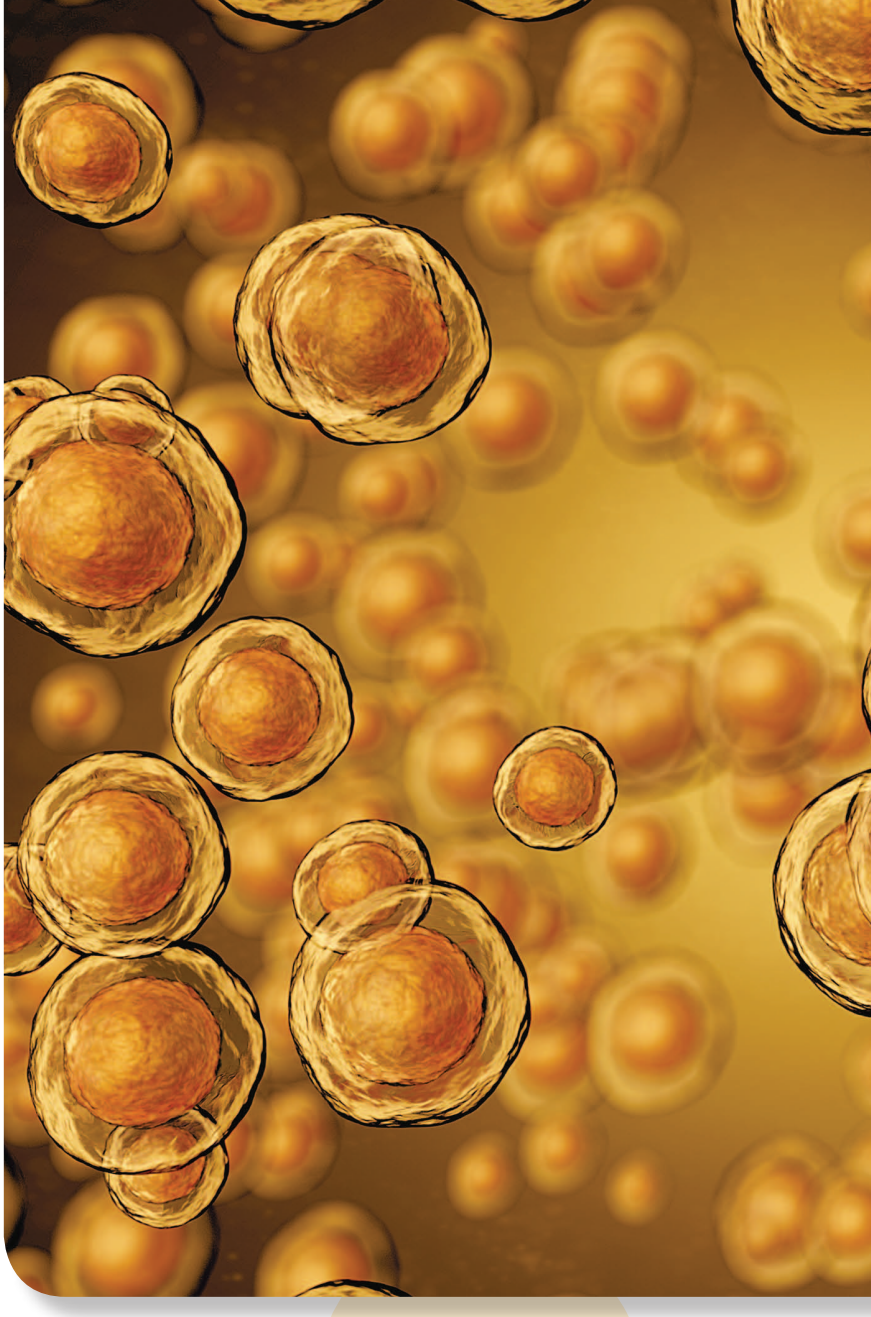

To address the difficulty of separating touching particles in an image, a method based on the area ratio of a circular mask is proposed in this article, and a framework consisting of image segmentation, concave point detection, point–pair matching, and the shape estimation of particles is implemented. A given color image is first preprocessed to obtain a binary image, then a corner detection algorithm is adopted to obtain a rough estimation of potential concave points, following which, the area ratio method is used to refine segmentation points qualified. The segmentation points obtained are matched to each pair by gray projection according to a certain evaluation criteria. Finally, each pair of points and one of their adjacent pixels on the border are used to estimate the status of each particle before adhesion, and the contour of each particle is generated using the curve fitting method. Experimental results show that the proposed method is consistent with human visual perception and can be used in the practice.

Separating Touching Particles

A Concavity-Based Method Using the Area Ratio of a Circular Mask

Digital Object Identifier 10.1109/MSMC.2018.2794559
Date of publication: 20 April 2018

2333-942X/18©2018IEEE

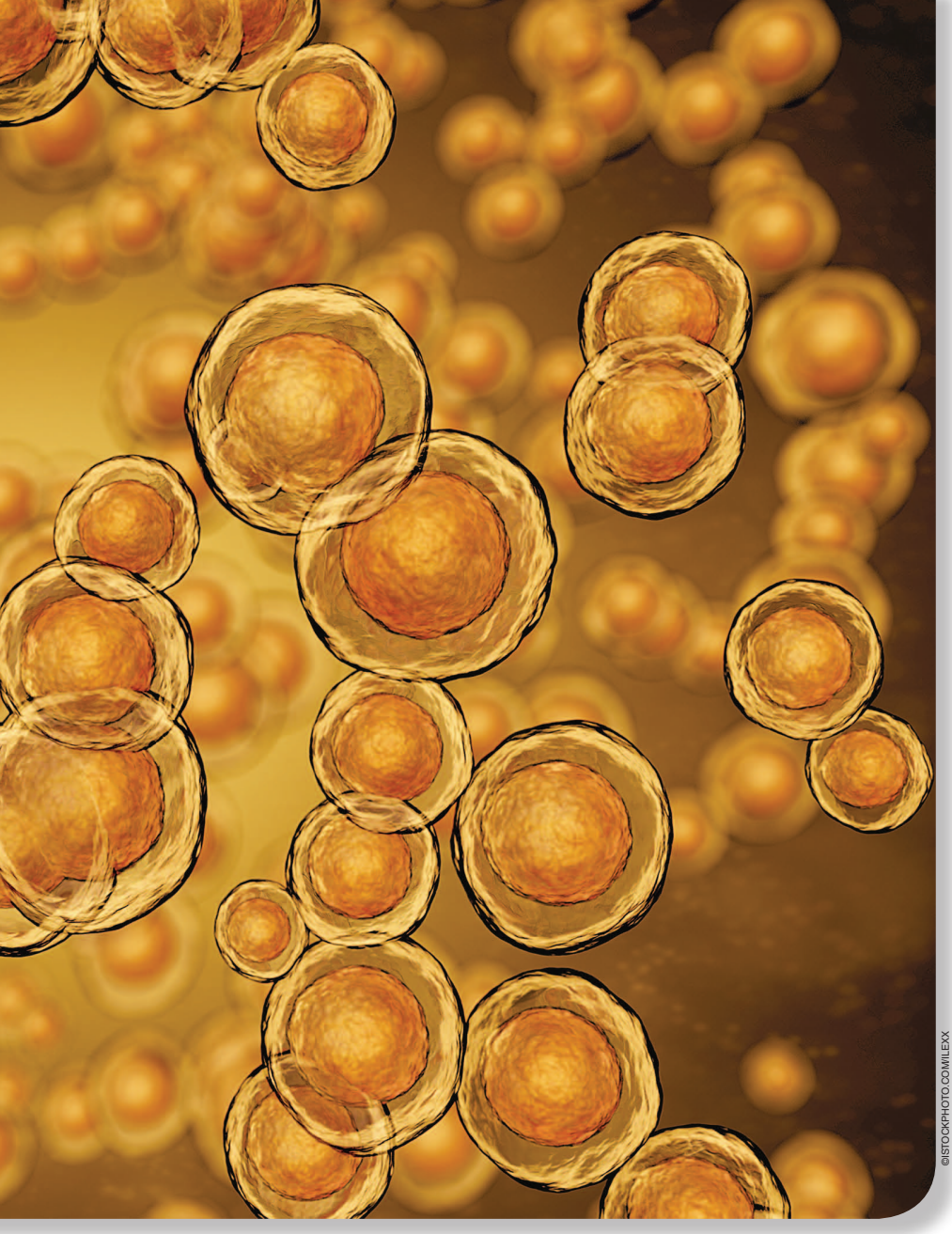

©ISTOCKPHOTO.COM/ILEXX

Image Processing

Image-based particle analysis is an important technique in the field of image processing. It is widely used in cell analysis [1], chromosome segmentation [2], pathogen detection [3], seed screening [4], nanoparticle segmentation [5], and rock analysis [6], among others. There is an obvious gray difference between the target and the background in an image, by which objects can be easily extracted from the background through the thresholding method. However, due to the contact, adhesion, or overlapping of each other, their contours mix together, affecting the accuracy of the parameter analysis. For example, in the biomedical field, cell counting and feature extraction are essential for the accurate diagnosis and prognosis of an expert system. Caused by overlapping cells in images, it is difficult to analyze the parameters quantitatively related to the number of cells, and it is crucial to split the overlapping cells into single ones.

Many techniques have been proposed in recent years to solve this problem, including the watershed-based method [9], the morphology method [10], the concavity analysis method [11], the active contour model [12], a level set algorithm [14], the Hough transform (i.e., the ellipse-fitting method) [16], [17], machine-learning methods [18], [22], and so on. As the classic segmentation algorithm for separating particles, the watershed-based method is well-suited for a large number of particles with similar shapes due to its fast calculations. However, if these particles differ in geometric size, the search for local extrema usually leads to oversegmentation [9], [19]. The improved methods, e.g., the marker watershed and rule-based watershed, solve the oversegmentation problem to some extent; however, they cannot address the problem of heavy overlapping. The morphological method involves separating objects by using a combination of dilation and erosion operations, which separates two touching objects; however, for clustered particles with a small concavity, it results in a large deviation [9]. Shape-based methods, e.g., the level set algorithm, detect the target object by minimizing the energy function, which does not rely on the edge information in the image and yields satisfactory edge extraction results from images with weak edges and noise [15]. The active contour model completes the segmentation of objects through the iterative computation of the energy function and extracts particles from a complex background to overcome the oversegmentation problem [12]. However, this method requires considerable computations as well as the initialization of complex parameters, which is unsuitable for the segmentation of a large number of particles. The Hough transform (ellipse-fitting method) assumes sufficient prior knowledge [16], [17] and sometimes requires template matching to determine particle contours for curve fitting, in addition to the boundary information of the particles [20]. Mainly used for round or elliptical particles and vulnerable to noise interference, the Hough transform involves complex computation, thereby limiting its application.

The concavity-based method searches for concave points as potential separating points, and from a geometrical perspective, it considers particle shape and contour information instead of gray information. For example, Ohta et al. [21] extracted the contour of each particle and used three points at intervals to form two vectors. They then calculated the vector angles and selected the minimum angle as a potential splitting point relative to the angle's proportion to concavity. This method ignores depth information that can easily succumb to interference. Kumar et al. proposed a rule-based approach for concave point analysis [22] in which a support vector machine (SVM) was used to screen the best separating line. This method is suitable for the segmentation of particles with varying shapes and sizes but needs a large number of training samples and can easily lead to the loss of key points in multipoint regions. Farhan et al. [23] improved the approach involving the combination of segmentation and key points but were unable to avoid excessive dependence on parameter settings and the oversegmentation problem [23]. LaTorre et al. [24] proposed a concavity point analysis-based clump splitting method by considering the holes in the clumps, in which two-step binarization is used for cell-particle extraction and the concave points are detected. The separating lines between the two particles are obtained by calculating the minimum distance. However, this method requires many parameters and its robustness is unsatisfied. Although these methods obtain satisfactory results in different applications, methods based on concave point analysis continue to face problems as a result of the complexity of adhesion and overlapping.

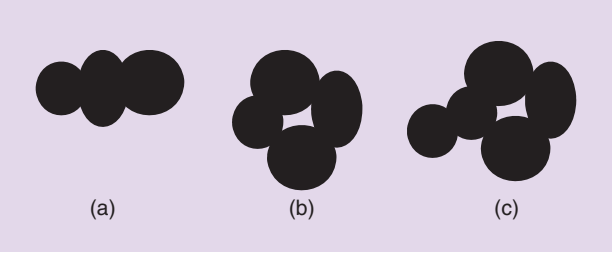

Figure 1. The touching types of particles: (a) series touching, (b) parallel touching, and (c) mixed touching.

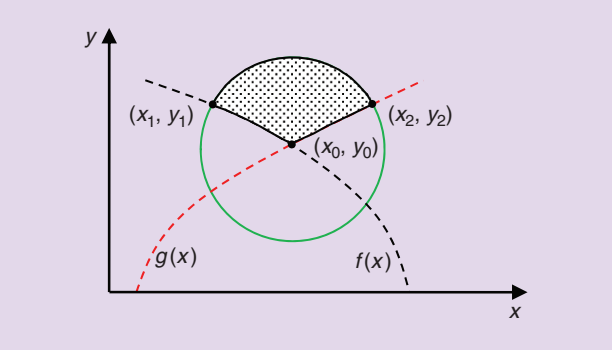

Figure 2. The intersection of two functions.

This article proposes an automatic segmentation method based on concave point analysis. The main contribution of this study is the discovery of the location of concave points, as well as the curve connection between concave points of touching particles.

Methodology

Concavity and convexity are important features of geometric figures. In the particle image, most individuals appear to be convex polygons, but when particles overlap, some concave shapes appear in the touching area, which leads to the particle mixing the convex and concave characteristics. The concave points are located in the concave region of the contour, and if the concave region is extracted, the concave points can be located easily and a separation line obtained. If there is touching or overlapping among particles, the forms can be categorized into series touching, parallel touching, and mixed touching, which are shown in Figure 1(a)–(c).

Irrespective of the type of touching, the touching region usually generates concave points. Touching involving three or more particles may be decomposed into a situation involving the adhesion of two particles. For the adhesion of the two particles, the boundary can be expressed as the intersection of functions $f(x)$ and $g(x)$, as shown in Figure 2, where the circle with radius R and center (x_0, y_0) is expressed as

$$(x-x_0)^2+(y-y_0)^2=R^2. \tag{1}$$

In other words, $y_0=f(x_0)=g(x_0)$, and the intersection of the circle and $f(x)$ is

$$y_1=f(x_1)=\sqrt{R^2-(x_1-x_0)^2}+y_0. \tag{2}$$

The intersection of the circle and $g(x)$ is

$$y_2=g(x_2)=\sqrt{R^2-(x_2-x_0)^2}+y_0. \tag{3}$$

To obtain the area of the shaded part of the circle, the integral function can be expressed as

$$S=\int_{x_1}^{x_0}\left[\sqrt{R^2-(x-x_0)^2}+y_0-g(x)\right] +\int_{x_0}^{x_2}\left[\sqrt{R^2-(x-x_0)^2}+y_0-f(x)\right]. \tag{4}$$

Since the area of a circle is

$$S_A=\pi R^2, \tag{5}$$

the area ratio of the shaded part and the circle is

$$\text{Ratio}'=\frac{S}{S_A}. \tag{6}$$

To describe the geometry of the two particles in the image, $f_0(x)$ and $g_0(x)$ are assumed to be two circles

with centers (a_1, b_1) and (a_2, b_2), and radii R_1 and R_2, respectively. That is,

$$f_0(x) = \sqrt{R_1^2 - (x - a_1)^2} + b_1 \tag{7}$$

and

$$g_0(x) = \sqrt{R_2^2 - (x - a_2)^2} + b_2. \tag{8}$$

If the two circles intersect, taking an intersection point of $f_0(x)$ and $g_0(x)$ as the circle center and R_3 as the radius, the area of the new circle, which does not overlap with $f_0(x)$ and $g_0(x)$, is expressed as S [the shaded area in Figure 3(a)]. The value of S, therefore, is less than half of the area of the circle.

According to the assumption whereby the graphical area in a plane space is invariant to rotation, the graphic in Figure 3(b) rotates and shifts its coordinates. Then, $f_0(x)$ and $g_0(x)$ can be changed to

$$x^2 + y^2 = R_1^2 \tag{9}$$

and

$$x^2 + (y - m)^2 = R_2^2. \tag{10}$$

To describe this relationship, a special case is used to solve the problem. Assuming the existence of two circles of equal area, the black circle is centered at (0, 0), the center of the red circle has the same horizontal coordinate as the black circle, and the radius of both is 1 (as shown in Figure 4). When the center of the red circle shifts from (1, 0) to (2, 0), the area ratio decreases from a reduction in the overlapping region and is always less than 0.5 when there is a concave point. The larger the degree of concavity, the smaller the area ratio; therefore, analyzing concave points using the method of area ratio is reasonable from a theoretical aspect, which is suitable for analyzing the situation of the deep adhesion of the particles.

In practical applications, the area overlapping two particles in a circle mask is calculated as

$$\text{Ratio} = 1 - \text{Ratio}' = 1 - \frac{S}{S_A}. \tag{11}$$

This ratio reflects the degree of concavity of the graphs.

A Framework for Particle Separation

Concave Point Detection

The method based on concave point analysis consists of three steps. To ensure accuracy and efficiency, a detection step based on a curvature scale space (CSS) corner detector and a refining step based on the area ratio are decomposed to determine the final position of the concave points.

The Screening of Concave Points

To overcome high computational costs, the CSS method is used for rough screening. The key steps are as follows:

- step 1: apply a Canny edge detector to process the input image, and obtain a binary edge-map
- step 2: extract the edge contours from the edge-map; fill in the gaps in the contours and find the T-junctions
- step 3: compute the curvature at a high scale σ_{high} for each edge contour
- step 4: consider those local maxima as initial corners whose absolute curvatures satisfy the criteria
- step 5: track the corners from the highest scale to the lowest scale to obtain a better position
- step 6: compare the T-junction to other corners, and remove one of the two corners that are very close.

An example of image preprocessing is shown in Figure 5, where (a) is the gray image, (b) is the binary image, (c) is the boundary contour image using a Canny edge operator, and (d) shows the results of corner detection using the CSS method, where the corners are marked with red boxes.

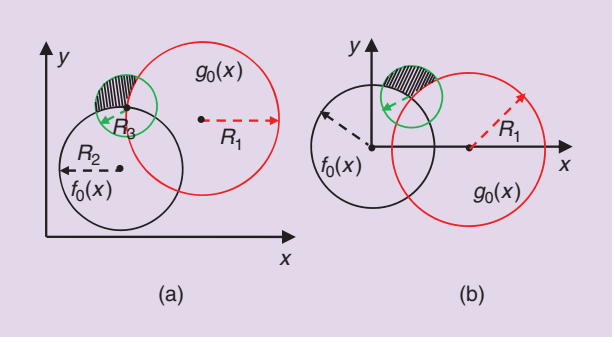

Figure 3. The intersection of two circles (a) before rotation and (b) after rotation.

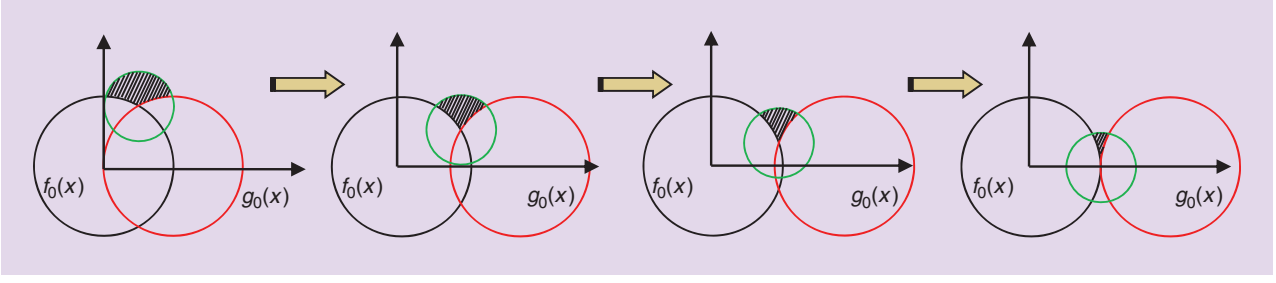

Figure 4. A flowchart of the proposed method.

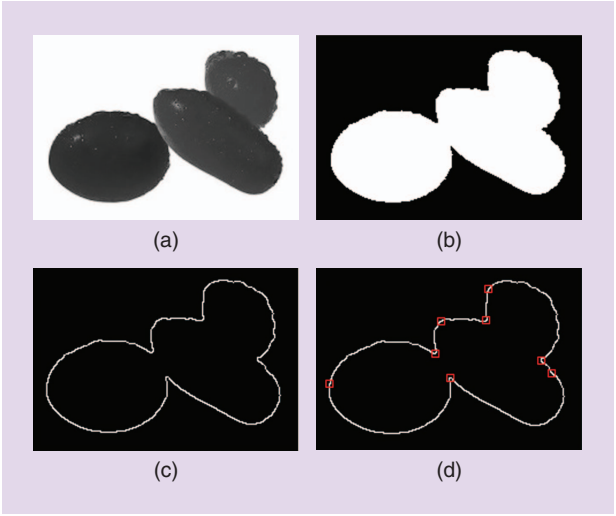

Figure 5. A sample of CCS corner detection: a (a) gray image, (b) binary image, (c) contour, and (d) the corners.

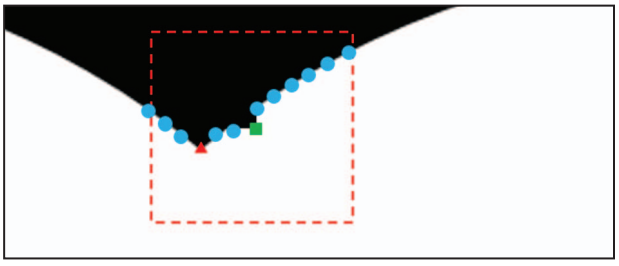

Figure 6. The refinement of a concave point in its neighborhood.

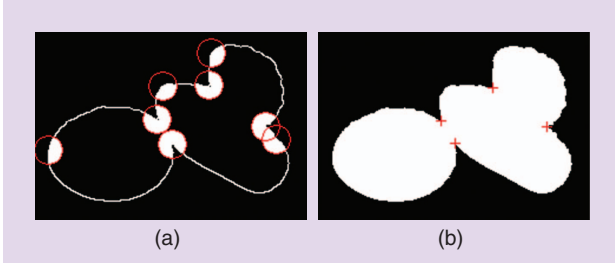

Figure 7. The result of concave point positioning: (a) a mask image and (b) the concave points location.

The Accurate Detection of Concave Points

The corners exist not only in the region overlapping the two particles but also in the convex point of the particles, which lie all along their contours. From the method based on the area ratio of a circular mask, convex points and some concave points with small concavity are filtered out, and the concave points for segmentation are then reserved. The relevant steps are as follows:

- step 1: obtain the index and coordinates of each corner, and set the radius of the circular mask according to particle size in actual situations
- step 2: take each corner coordinate as the center of the circular mask, and cut out the region through an AND operation between the mask and the particle image
- step 3: calculate the number of white pixels as the area, which corresponds with the particle region; if there are many white regions, the largest area should be selected
- step 4: compute the area ratio of the white area in the circular mask
- step 5: select the points with the largest area ratios as the candidate separating points according to the estimated number of particles
- step 6: refine each candidate point in its neighboring region.

For each candidate point obtained from step 5, the points along the boundary are selected in its $[m \times m]$ neighboring pixel region; these points are used to calculate the area ratios, and the maximum ratio is selected as the final concave point. This underlying principle is shown in Figure 6. Suppose the green rectangular point to be the concave point from step 5; the red-dotted square is in the neighborhood of the concave point, and the blue circular points represent the other points on the contour of particles. Taking each of these points as the center of the circle to calculate the area ratio according to steps 2–5, the final concave point with the maximum area ratio is selected. As shown in Figure 6, the final concave point chosen is the red point rather than the green point.

A sample of the positioning of concave points is shown in Figure 7, where (a) shows the area ratio of the mask image, the red circle is the mask, and the white area in the red circle represents the particle area. Figure 7(b) shows the final result, and the four concave points are marked with a plus (+) sign.

Concave Point Pairing

Concave point pairing is intended to determine the concave point pair for the segmentation of two particles, which is the premise for performing an accurate line segmentation. Since the two particles adhere to one another, a concavity phenomenon appears in the contact parts, which imbues the pattern of the adhered particle with the characteristic of a concave graph [26]. Gray projection is, therefore, used for matching, i.e., cutting the region into a specific size consisting of two concave points as the candidate point pair; the gray projection then proceeds in vertical and horizontal directions, respectively. Finally, the two concave points are assessed to determine whether they belong to a pair according to specific rules.

When gray projection is implemented onto the image extended from the connection between concave points (according to prior knowledge of a concave point pair), the projection curve along with the connection line indicates that the middle value is smaller than the end point values; whereas, the vertical projection curve indicates that the middle value is larger than the end point values.

This is shown in Figure 8, where the red rectangle is the region containing a pair of concave points, and the upper and right regions contain the gray projection of the rectangular region.

Segmentation Line Construction

Conventional methods for segmenting two touching particles involve connecting paired concave points directly through a line, as shown in [18], [20], and [22]. This method is simple, intuitive, and can directly separate adhesive particles, it does not, however, fit the cognitive law of human vision. Regardless of the touching types, the touching border cannot be a straight line; therefore, the geometric status of each particle prior to touching must be estimated. Since the particles analyzed in this study are convex, they can be estimated based on the concave point pair obtained and other points on the given object.

According to geometrical principle, three noncollinear points can only form one circle. For individual particles, the concave points and boundary points are known; thus, making use of the two end points of the dividing line and any other point along its edge, we can achieve a three-point circle fitting. We adopt the perpendicular bisector intersection method, i.e., two straight lines connecting three points, with the intersection of their perpendicular bisectors being the center of a circle, and the distance between the center and any of the three points being the radius. Its geometric model is shown in Figure 9, where A, B, and C are the three points in the same plane, and their coordinates are (x_a, y_a), (x_b, y_b), and (x_c, y_c), respectively.

Based on these principles, the processing steps involved in arc fitting are as follows:

- step 1: collect the contour coordinates of the individual particles split using a straight line between two concave points, and mark the two separating points A and B
- step 2: obtain points C and D from the contour coordinates that are near points A and B, respectively, but do not belong to the straight line connecting A and B
- step 3: fit circles with points A, B, and C, and A, B, and D, respectively, and obtain the centers and radii of the two circles
- step 4: get arcs Arc_{AB} and Arc'_{AB} of the two circles according to the spatial relationship between the circle centers and the splitting points
- step 5: fill the regions encircled by arcs and segmentation lines with pixel value 1, and calculate areas S_{AB} and S'_{AB} of the two regions
- step 6: compare S_{AB} and S'_{AB}, and choose the smaller of the two as the compensation part of the particle.

Experimental Results

To evaluate the proposed method, several particle images from different conditions were employed for an experiment. The experimental results showed that the proposed method is better than some traditional segmentation methods.

A Comparison of Methods

In this article, the ultimate erosion method [25] and marker watershed method [27] were used for comparison with the proposed method. Some experimental results are shown in Figure 10, where the blue contours represent the markers after separation. Figure 10(a) and (e) shows three types of original particle images of different sizes on different rows, and Figure 10(b) and (f) shows the results obtained by the ultimate erosion method. Figure 10(b) and (f) indicates that most touching particles could be split [only Figure 10(b) exhibits undersegmentation], but restoring the original shape before erosion is difficult. Figure 10(c) and (g) shows the results of the marker watershed method, and although it eased oversegmentation to some extent, it could not avoid it entirely, and false separations exist in Figure 10(g). For images in Figure 10(d) and (h), the shape of every particle was estimated based on the accurate detection of the splitting points, which is consistent with the law of human visual perception. To test the robustness of our proposed method, the effect of noise on the concave points positioning and point–pair matching was analyzed.

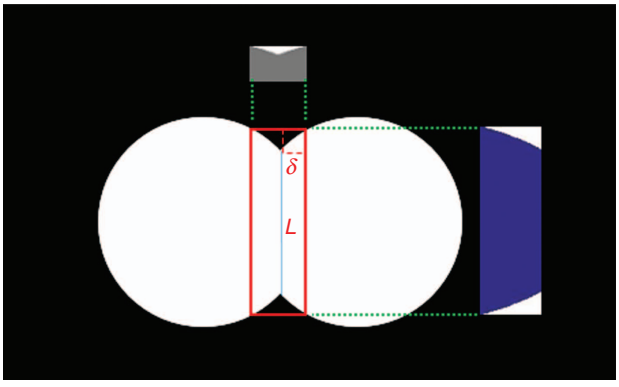

Figure 8. The gray projection of an image with two concave points.

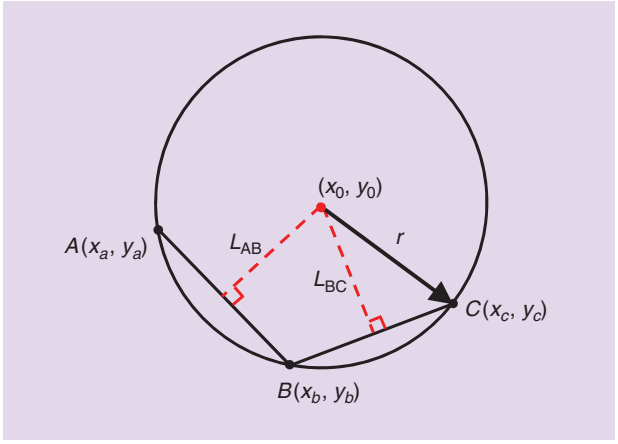

Figure 9. The geometric model of a three-point circle fitting.

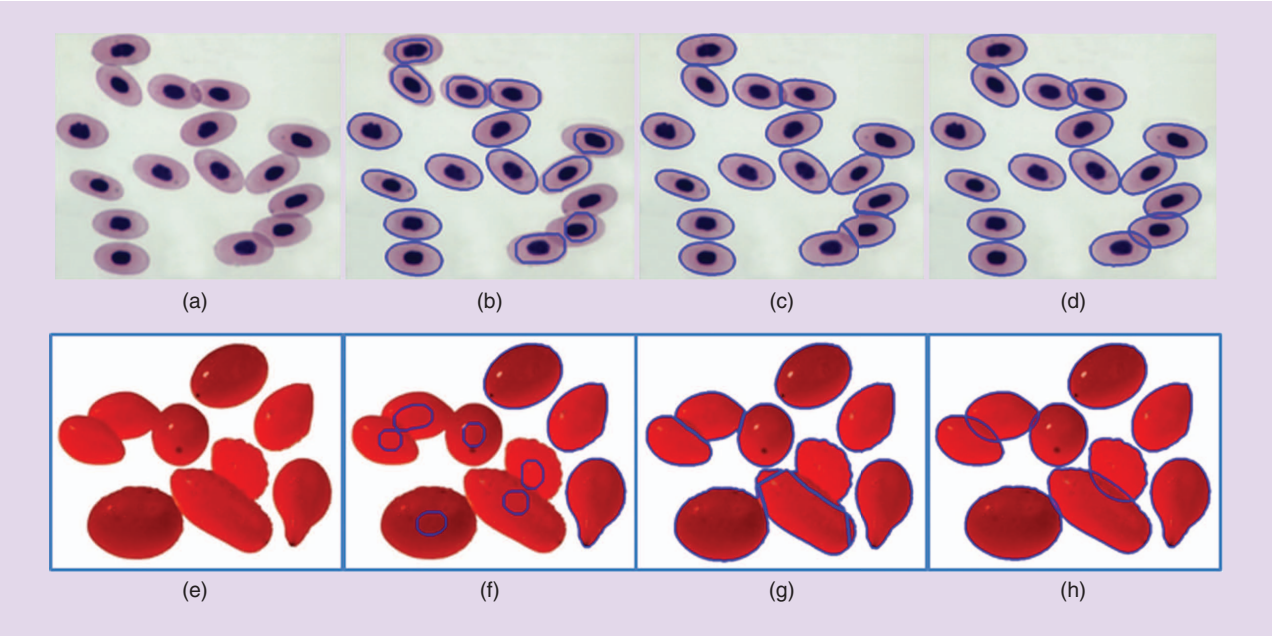

Figure 10. (a)–(h) Comparisons of the experimental results: the (a) and (e) original images, (b) and (f) ultimate erosion method, (c) and (g) marker watershed method, and (d) and (h) proposed method. The blue contours represent the markers after separation.

The Influence of Noise on Concave Point Positioning

As the contours of the actual adhesion area are not always smooth, and traditional algorithms are vulnerable to the interference of rugged borders, many microdents may be mistakenly considered to be splitting points (pseudosplitting points). Although curve smoothing can reduce noise, it also leads to the loss of important data and affects positioning accuracy. Since smoothing blunts corners and inappropriate parameter adjustments may lead to the disappearance of corners altogether, the concave points cannot be precisely located. The method proposed in this article uses the corner detector for rough screening, it then uses the area ratio of the circular mask for refinement, which is not sensitive to small convex and concave points, and is therefore robust.

Figure 11(a) displays the image in Figure 5(b) distorted with noise, which increased the number of small convex and concave points along the boundary. Figure 11(b) is the result of corner detection; compared to the image in Figure 5(d), the number of corners increased considerably. The image in Figure 11(c) shows circular masks according to corners, and Figure 11(d) displays the final result of

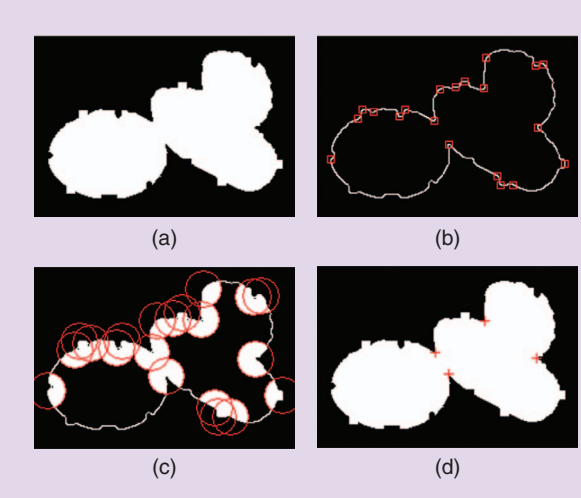

Figure 11. The influence of noise on concave point positioning: (a) a binary image with noise, (b) the result of corner detection, (c) the circular masks in an image, and (d) the location of the splitting points.

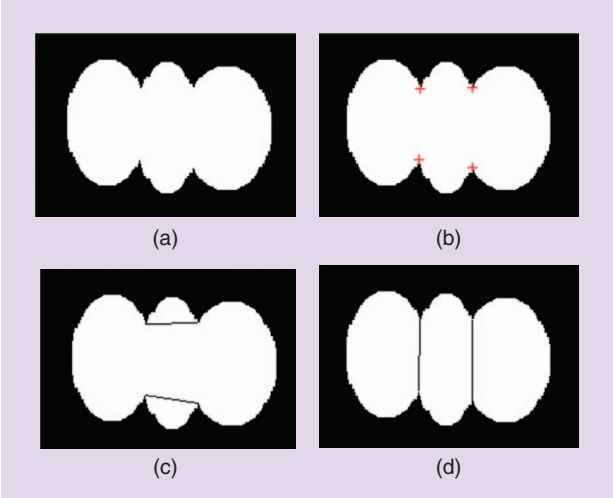

Figure 12. The results of point-pair matching: (a) a binary image, (b) the concave points location, (c) the shortest-distance method, and (d) the proposed method.

concave point detection. As seen in the graph, our method can accurately locate splitting points, and it is robust against noise.

Point–Pair Matching Accuracy

After concave point detection, matching is not required for adhesion between two particles. However, in the case of three or more particles, the structure is composed of complex touching areas. Even if the true concave points can be determined, once there is a matching error, the method remains unable to construct the correct separation line. A commonly used matching method is the shortest-distance algorithm [26], which uses the characteristic of the candidate point pair having the shortest distance due to concavity. For most circular shapes, it works well; however, for long elliptical particles, it easily results in matching errors. As shown in Figure 12, (a) is the binary image; (b) is the result of concave point detection, where the concave points are marked with a plus (+) sign; (c) is the result of matching using the shortest-distance method; and (d) is the result obtained by using the proposed method. From this, we see that the direct use of the shortest-distance method is not suitable for concave point–pair matching of elliptical particles, and the proposed method based on the gray projection of concave regions is more robust.

A commonly used matching method is the shortest-distance algorithm, which uses the characteristic of the candidate point pair having the shortest distance due to concavity.

Accuracy Analysis

After matching the point pair, traditional methods use a straight line to separate particles by connecting two concave points, as shown in [18], [20], [22], and [27]. To objectively evaluate the accuracy of this, we used the matting function in Adobe Photoshop to manually cut out individual particle regions and compare the proposed method with traditional methods using the difference ratio

$$\eta = S_D/S_T, \tag{12}$$

where S_D is the difference between the results of the proposed method and standard value, and S_T is the standard deviation obtained by manual segmentation, i.e., those that were calculated by the number of pixels). The smaller the value of η, the better the segmentation performance.

Table 1 displays the quantitative comparison of accuracy. Of these, rows two, three, and four show the η values of the three single particles, and the fifth line shows the comprehensive evaluation of the three particles. Table 1 indicates that the proposed method had less impact than the traditional method on those particles. The comprehensive error rate of 3.41% was only one-third of the traditional method, indicating that the proposed method was effective in separating the overlapping particles, and its separating curve was more accurate than that of traditional straight segmentation.

Table 1. A quantitative comparison of accuracy.

Image	η Value Derived by Traditional Method	η Value Derived by Proposed Method
Particle 1	6.50%	0.77%
Particle 2	16.59%	8.90%
Particle 3	8.36%	1.51%
Comprehensive	10.13%	3.41%

Conclusion

In this article, a concave point analysis method using the area ratio of a circular mask was proposed, and a framework consisting of concave point detection, point–pair matching, and the status estimation of particles was developed on the basis of human vision perception. Experiments showed that the method is in accordance with human vision perception and is particularly suitable for the segmentation of overlapping particles, which could be adapted for use in a wide variety of fields. However, due to excessive dependence on concave points, it is difficult for the method to process multiple particles without concave points. Therefore, developing a more adaptable approach by considering color and texture features to improve its robustness will be the scope of our research in the future.

Acknowledgments

This work was supported by the National Natural Science Foundation of China (No. 61403283), the Shandong Provincial Natural Science Foundation (No. ZR2013FQ036), and the Technology Development Plan of Weifang City (No. 201301015).

About the Authors

Wencheng Wang (wwcwfu@126.com) earned his Ph.D. degrees in pattern recognition and intelligent systems from Shandong University, Jinan, China, in 2011. He is currently a professor with the College of Information and Control Engineering, Weifang University, China, and serves as an associate editor of *Transactions of the Institute of Measurement and Control*. His research group has published more than 40 papers in academic journals. His current research interests include computer vision and pattern recognition. He is a Member of the IEEE.

Xiaohui Yuan (xiaohui.yuan@unt.edu) earned his Ph.D. degree in computer science from Tulane University, New Orleans, Louisiana, in 2004. He joined the University of North Texas, Denton, as an assistant professor in 2006 and became an associate professor in 2012. He has served on the editorial board of several international journals and as a session chair at many conferences. His current research interests include computer vision, machine learning, and artificial intelligence, and his research findings have been published in more than 70 peer-reviewed papers. He is a Member of the IEEE.

Xiaojin Wu (wfuwxj@163.com) earned his Ph.D. degree in control science and engineering from Beijing Jiaotong University, China, in 2011. He is currently with the College of Information and Control Engineering, Weifang University, China, and has published more than ten papers in academic journals. His current research interests include computer vision, intelligent systems, and image processing.

Tao Ji (jtsdu@126.com) earned his Ph.D. degree in control science and engineering from Shandong University, China, in 2006. He is currently a professor with the College of Information and Control Engineering at Weifang University, China, and has published more than 30 papers in academic journals. His current research interests include intelligent control and information processing.

Lin Feng (felincity@qq.com) earned her Ph.D. degree in computer science from the Hefei University of Technology, China, in 2014, where she is currently an associate professor. Her current research interests include vehicular ad hoc networks, wireless networks, and computer vision.

References

[1] H. Kong, M. Gurcan, and K. Belkacem-Boussaid, "Partitioning histopathological images: An integrated framework for supervised colour–texture segmentation and cell splitting," *IEEE Trans. Med. Imag.*, vol. 30, no. 9, pp. 1661–1677, 2011.

[2] Y. Zhao, X. Wu, S. G. Kong, and L. Zhang, "Joint segmentation and pairing of multispectral chromosome images," *Pattern Anal. Applicat.*, vol. 16, no. 4, pp. 497–506, 2013.

[3] S. Brandes, Z. Mokhtari, F. Essig, K. Hünniger, O. Kurzai, and M. T. Figge, "Automated segmentation and tracking of non–rigid objects in time–lapse microscopy videos of polymorphonuclear neutrophils," *Med. Image Anal.*, vol. 20, no. 1, pp. 34–51, 2015.

[4] P. Lin, Y. M. Chen, Y. He, and G. W. Hu, "A novel matching algorithm for splitting touching rice kernels based on contour curvature analysis," *Comput. Electron. Agriculture*, vol. 109, pp. 124–133, Nov. 2014.

[5] M. Jungmann, H. Pape, P. Wisskirchen, C. Clauser, and T. Berlage, "Segmentation of thin section images for grain size analysis using region competition and edge–weighted region merging," *Comput. Geosci.*, vol. 72, pp. 33–48, Nov. 2014.

[6] W. Wang, X. Yuan, X. Wu, and Y. Liu, "Fast image dehazing method based on linear transformation," *IEEE Trans. Multimedia*, vol. 19, no. 6, pp. 1142–1155, 2017.

[7] Z. Cao, X. Liu, N. Gu, S. Nahavandi, D. Xu, C. Zhou, and M. Tan, "A fast orientation estimation approach of natural images," *IEEE Trans. Syst., Man, Cybern. Syst.*, vol. 46, no. 11, pp. 1589–1597, 2016.

[8] W. Wang, X. Yuan, X. Wu, and Y. Liu, "Dehazing for images with large sky region," *Neurocomputing*, vol. 238, pp. 365–576, May 2017.

[9] H. Yang and N. Ahuja, "Automatic segmentation of granular objects in images: Combining local density clustering and gradient–barrier watershed," *Pattern Recognit.*, vol. 47, no. 6, pp. 2266–2279, 2014.

[10] D. Yu, T. D. Pham, and X. Zhou, "Analysis and recognition of touching cell images based on morphological structures," *Comput. Biol. Med.*, vol. 39, no. 1, pp. 27–39, 2009.

[11] M. Farhan, O. Yli-Harja, and A. Niemistö, "A novel method for splitting clumps of convex objects incorporating image intensity and using rectangular window-based concavity point–pair search," *Pattern Recognit.*, vol. 46, no. 3, pp. 741–751, 2013.

[12] M. E. Plissiti and C. Nikou, "Overlapping cell nuclei segmentation using a spatially adaptive active physical model," *IEEE Trans. Image Process.*, vol. 21, no. 11, pp. 4568–4580, 2012.

[13] S. Arslan, T. Ersahin, R. Cetin-Atalay, and C. Gunduz-Demir, "Attributed relational graphs for cell nucleus segmentation in fluorescence microscopy images," *IEEE Trans. Med. Imag.*, vol. 32, no. 6, pp. 1121–1131, 2013.

[14] Z. Lu, G. Carneiro, and A. P. Bradley, "An improved joint optimisation of multiple level set functions for the segmentation of overlapping cervical cells," *IEEE Trans. Image Process.*, vol. 24, no. 4, pp. 1261–1272, 2015.

[15] X. Qi, F. Xing, D. J. Foran, and L. Yang, "Robust segmentation of overlapping cells in histopathology specimens using parallel seed detection and repulsive level set," *IEEE Trans. Biomed. Eng.*, vol. 59, no. 3, pp. 754–765, 2012.

[16] N. Kharma, H. Moghnieh, J. Yao, Y. P. Guo, A. Abu-Baker, J. Laganiere, G. Rouleau, and M. Cheriet, "Automatic segmentation of cells from microscopic imagery using ellipse detection," *Inst. Eng. Tech. Image Process.*, vol. 1, no. 1, pp. 39–47, 2007.

[17] H. Xu, C. Lu, and M. Mandal, "An efficient technique for nuclei segmentation based on ellipse descriptor analysis and improved seed detection algorithm," *IEEE J. Biomed. Health Inform.*, vol. 18, no. 5, pp. 1729–1741, 2014.

[18] S. Nazlibilek, D. Karacor, T. Ercan, M. H. Sazli, O. Kalender, and Y. Ege, "Automatic segmentation, counting, size determination and classification of white blood cells," *Measurement*, vol. 55, pp. 58–65, Sept. 2014.

[19] P. Karvelis, A. Likas, and D. I. Fotiadis, "Identifying touching and overlapping chromosomes using the watershed transform and gradient paths," *Pattern Recognit. Lett.*, vol. 31, no. 16, pp. 2474–2488, 2010.

[20] G. Diaz, F. Gonzalez, and E. Romero, "Automatic clump splitting for cell quantification in microscopical images," in *Progress in Pattern Recognition, Image Analysis and Applications*, L. Rueda, D. Mery, and J. Kittler, Eds. Berlin: Springer–Verlag, 2007, pp.763–772.

[21] J. Ohta, F. Mayinger, O. Feldmann, and P. Gebhard, "An algorithm for evaluating overlapping bubble images recorded by double pulsed laser holography," *J. Visualisation*, vol. 4, no. 3, pp. 285–298, 2001.

[22] S. Kumar, S. H. Ong, S. Ranganath, T. C. Ong, and F. T. Chew, "A rule-based approach for robust clump splitting," *Pattern Recognit.*, vol. 39, no. 6, pp. 1088–1098, 2006.

[23] M. Farhan, O. Yli-Harja, and A. Niemisto, "An improved clump splitting method for convex objects," in *Proc. Seventh Int. Workshop Computational Systems Biology*, 2010, pp. 35–38.

[24] A. LaTorre, L. Alonso-Nanclares, S. Muelas, J. M. Peña, and J. DeFelipe, "Segmentation of neuronal nuclei based on clump splitting and a two-step binarization of images," *Expert Syst. Applicat.*, vol. 40, no. 16, pp. 6521–6530, 2013.

[25] J. Huang, "An improved algorithm of overlapping cell division," in *Proc. 2010 Int. Conf. Intelligent Computing and Integrated Systems*, pp. 687–691.

[26] X. Yuan, J. Guo, X. Hao, and H. Chen, "Traffic sign detection via graph–based ranking and segmentation algorithms," *IEEE Trans. Syst. Man, Cybern. Syst.*, vol. 45, no. 12, pp. 1509–1521, 2015.

[27] C. Jung and C. Kim, "Segmenting clustered nuclei using H–minima transform–based marker extraction and contour parameterisation," *IEEE Trans. Biomed. Eng.*, vol. 57, no. 10, pp. 2600–2604, 2010.

[28] W. Wang, X. Yuan, and S. Tang, "Touching particles separation based on area ratio of circular mask," in *Proc. 36th Chinese Control Conf.*, 2017, pp. 2043–2046.

SMC